# *Usp12 stabilizes the T-cell receptor complex at the cell surface during signaling*



**Citation:** Jahan, Akhee S. et al. "Usp12 Stabilizes the T-Cell Receptor Complex at the Cell Surface during Signaling." Proceedings of the National Academy of Sciences 113.6 (2016): E705–E714. © 2016 National Academy of Sciences

**As Published:** http://dx.doi.org/10.1073/pnas.1521763113

**Publisher:** National Academy of Sciences (U.S.)

**Persistent URL:** http://hdl.handle.net/1721.1/106472

**Version:** Final published version: final published article, as it appeared in a journal, conference proceedings, or other formally published context

PNAS PLUS

# Usp12 stabilizes the T-cell receptor complex at the cell surface during signaling

Akhee S. Jahan[a,1], Maxime Lestra[a,1], Lee Kim Swee[b,1,2], Ying Fan[a], Mart M. Lamers[a], Fikadu G. Tafesse[b,3], Christopher S. Theile[b], Eric Spooner[b], Roberto Bruzzone[a,c], Hidde L. Ploegh[b,d], and Sumana Sanyal[a,c,4]

[a]HKU-Pasteur Research Pole and Center for Influenza Research, School of Public Health, LKS Faculty of Medicine, University of Hong Kong, Hong Kong; [b]Whitehead Institute for Biomedical Research, Cambridge, MA 02142; [c]Department of Cell Biology and Infection, Institut Pasteur, 75015 Paris, France; and [d]Department of Biology, Massachusetts Institute of Technology, Cambridge, MA 02142

Edited by Arthur Weiss, University of California, San Francisco, CA, and approved December 24, 2015 (received for review November 5, 2015)

**Posttranslational modifications are central to the spatial and temporal regulation of protein function. Among others, phosphorylation and ubiquitylation are known to regulate proximal T-cell receptor (TCR) signaling. Here we used a systematic and unbiased approach to uncover deubiquitylating enzymes (DUBs) that participate during TCR signaling in primary mouse T lymphocytes. Using a C-terminally modified vinyl methyl ester variant of ubiquitin (HA-Ub-VME), we captured DUBs that are differentially recruited to the cytosol on TCR activation. We identified ubiquitin-specific peptidase (Usp) 12 and Usp46, which had not been previously described in this pathway. Stimulation with anti-CD3 resulted in phosphorylation and time-dependent translocation of Usp12 from the nucleus to the cytosol. Usp12$^{-/-}$ Jurkat cells displayed defective NFκB, NFAT, and MAPK activities owing to attenuated surface expression of TCR, which were rescued on reconstitution of wild type Usp12. Proximity-based labeling with BirA-Usp12 revealed several TCR adaptor proteins acting as interactors in stimulated cells, of which LAT and Trat1 displayed reduced expression in Usp12$^{-/-}$ cells. We demonstrate that Usp12 deubiquitylates and prevents lysosomal degradation of LAT and Trat1 to maintain the proximal TCR complex for the duration of signaling. Our approach benefits from the use of activity-based probes in primary cells without any previous genome modification, and underscores the importance of ubiquitin-mediated regulation to refine signaling cascades.**

Usp12 | TCR signaling | deubiquitylases

Regulation of immune signaling cascades through posttranslational modification by ubiquitin (Ub) and Ub-like small molecules is being increasingly recognized (1–5). As with many innate immune signaling cascades, such as Toll-like receptors and nucleotide-binding domain and leucine-rich repeat-containing receptors, ubiquitylation plays a significant role in the adaptive immune responses (6–8). T cells respond to T-cell receptor (TCR) engagement by triggering a plethora of rapid cytosolic events, including several modifications such as phosphorylation, ubiquitylation, and neddylation, ultimately resulting in nuclear translocation of NFκB (1, 9, 10). With the advent of more sophisticated techniques, the model for TCR signaling is being progressively refined (11–13). The current consensus supports that signaling is initiated by ligation of a peptide/MHC complex to activate TCR-associated Src/Syk family kinases. Signaling complexes are formed with their adaptor proteins, such as LAT, to form discrete clusters that trigger downstream phosphorylation (14, 15). Advanced electron microscopy and single molecule techniques have shed light on the dimension and composition of these TCR microclusters at the immunological synapse (16–18).

TCR signaling to NFκB requires assembly of large multiprotein complexes comprising several kinases, scaffold proteins, Ub ligases, and deubiquitylating enzymes (19, 20). The TCR forms a multisubunit complex with CD3 consisting of cytoplasmic immunoreceptor tyrosine-based activation motifs. A series of phosphorylation events that involves PI3K and PDK1 culminates in PKC phosphorylation. The NEMO/IκB (IKK) complex integrates signals from upstream stimuli and results in NFκB activation. Several studies have identified key signal mediators involved in the pathway, including Zap70, SLP-76, PLC, Fyn, Lck, PKC, Vav1, Bcl10, Malt1, and Carma1. Biochemical characterization of these effectors has suggested a putative sequence of events whereby PKC activity is followed by nucleation of the multiprotein Carma-Bcl10-Malt complex within lipid microdomains to recruit the inhibitor of NFκB kinase, IKK. The signal initiated by these core events is then disseminated through adaptor proteins, such as LAT and SLP-76, to ultimately induce global changes in gene transcription and facilitate effector functions.

Reports on the dynamics of TCR surface expression suggest that in accordance with other receptors, the TCR is internalized and recycled rapidly with a rate constant of ∼0.01 min$^{-1}$ (21). Additional evidence on Ub modification of the TCR-CD3 complex has revealed a tight regulation of TCR expression on immature T cells, critical for T-cell development (22). Ligation causes an intracellular retention, although the kinetics of internalization remains unaffected. Despite scant evidence on the mechanism of surface dynamics of TCR, available data on well-characterized receptors, such as the transferrin receptor and epidermal growth factor receptor, indicate that internalization and recycling occurs via a dynamic interplay between monoubiquitylation and deubiquitylation processes (23–25). Several enzymes of the ubiquitylation machinery have been reported to play a crucial

## Significance

We used an unbiased screening strategy to capture deubiquitylases that participate in T cell receptor signaling in primary cells under physiological settings. We identified ubiquitin-specific peptidase (Usp) 12 as a crucial component of TCR expression at the cell surface, and found supporting evidence for its function by creating an inducible genetic knockout in Jurkat cells. Using proximity-based labeling, we identified LAT and Trat1 as substrates of Usp12. In Usp12-deficient cells, both LAT and Trat1 are ubiquitin-modified and lysosomally degraded, thus down-regulating TCR surface expression. Our data define a role of Usp12 in the TCR signaling pathway for the first time, to our knowledge. These results underscore the importance of deubiquitylases in fine-tuning signaling cascades and provide a basis for the screening of small molecules to identify potential inhibitors.

Author contributions: A.S.J., M.L., L.K.S., F.G.T., and S.S. designed research; A.S.J., M.L., L.K.S., Y.F., M.M.L., F.G.T., C.S.T., E.S., and S.S. performed research; R.B. and H.L.P. contributed new reagents/analytic tools; A.S.J., M.L., L.K.S., M.M.L., and S.S. analyzed data; and L.K.S. and S.S. wrote the paper.

The authors declare no conflict of interest.

This article is a PNAS Direct Submission.

[1]A.S.J., M.L., and L.K.S. contributed equally to this work.

[2]Present address: BiomedX Innovation Center, 69120 Heidelberg, Germany.

[3]Present address: Ragon Institute of MGH, MIT, and Harvard, Cambridge, MA 02139.

[4]To whom correspondence should be addressed. Email: sanyal@hku.hk.

This article contains supporting information online at www.pnas.org/lookup/suppl/doi:10.1073/pnas.1521763113/-/DCSupplemental.

role in orchestrating maturation, differentiation, and function of T cells (26, 27). Among the well documented of these are TRAF6 (28, 29), Cbl-b (9, 30), ITCH (9), GRAIL, and the SOCS proteins of the E3 ligase family and CYLD (1, 31), ubiquitin-specific peptidase (USP) 9X (32, 33), and A20 (6, 34) from the deubiquitylase (DUB) family. Adding another layer of complexity is the diverse array of Ub chain linkages that dictate the outcome of such modifications in the context of cellular responses such as localization, degradation, and signaling (35, 36).

Here we used an activity-based probe to target functional DUBs in the TCR signaling pathway. We used a C-terminally modified Ub with vinyl methyl ester (VME) to capture DUBs that are recruited to the cytosol on TCR activation in both mouse T lymphocytes and Jurkat cells. On stimulation with anti-CD3 antibodies followed by large-scale immunoprecipitation, we identified a set of cytosolic DUBs, including CYLD and Usp9X, that have been described in the context of TCR signaling (28, 32). Among those that were differentially captured, Usp12 and Usp46 displayed a significant increase in recovery from TCR stimulated cells compared with resting cells. Usp12 localizes primarily to the nucleus, but was enriched in the cytosol on stimulation. Usp12$^{-/-}$ Jurkat cells generated through Cas9/CRISPR-mediated genome editing were defective in NFκB and NFAT activities as well as TCR expression at the cell surface. Reconstituted HA-Usp12 in knockout cells rescued this phenotype. Through proximity-based labeling with a promiscuous BirA-ligase fused to Usp12 (BirA*-Usp12), we identified LAT and Trat1 as substrates. Both undergo mono-Ub modification and are lysosomally degraded in Usp12$^{-/-}$ cells. Our results indicate that Usp12 acts directly on these adaptor proteins to stabilize the TCR complex at the cell surface for the duration of signaling.

## Results

**Capturing DUBs Recruited During TCR Signaling.** To identify DUBs that are specifically recruited on TCR activation, we used the experimental setup illustrated in Fig. 1*A*. T cells isolated from C57BL/6 WT mice were stimulated with anti-CD3 in the presence of HA-Ub-VME, followed by permeabilization in 0.1% Nonidet P-40. Control cells were treated in parallel without anti-CD3 antibodies. Supernatants enriched in the cytosolic fraction were separated from pellets, comprising nuclear material and unbroken membranes. HA-reactive material was visualized by immunoblotting with HRP-conjugated anti-HA antibodies. Distinct profiles in the two lanes indicate differential recovery of HA-Ub-VME–reactive DUBs in the cytosol fractions in resting vs. TCR-stimulated samples (Fig. 1*B*). Jurkat cells displayed a similar phenomenon on TCR activation, although the bulk protein profiles appeared distinctly different from those of primary T cells (Fig. 1*B*).

To confirm that TCR stimulation and signaling occurred on treatment with anti-CD3 antibody, total phosphorylation profiles were visualized in control and stimulated samples using anti-phosphotyrosine (anti-pY) antibodies. As reported previously, time-dependent phosphorylation as well as dephosphorylation events were observed in stimulated samples for both T lymphocytes and Jurkat cells (Fig. 1*C* and Fig. S1*A*).

**Identification of DUBs Recruited on TCR Stimulation.** To identify the DUBs recruited specifically on TCR stimulation, we scaled up the experimental strategy described above for silver staining and mass spectrometry. HA-Ub-VME forms an irreversible covalent linkage with the Ub conjugation machinery, and modified DUBs can be effectively isolated by immunoprecipitation on anti-HA antibodies. The optimal concentration of HA-Ub-VME for immunoprecipitation was determined at a small scale using primary T cells, followed by isolation on conjugated anti-HA antibodies (Fig. 2*A* and Fig. S1*B*). For silver staining, 110 × 10$^6$ cells isolated from four C57BL/6 WT mice were distributed equally and

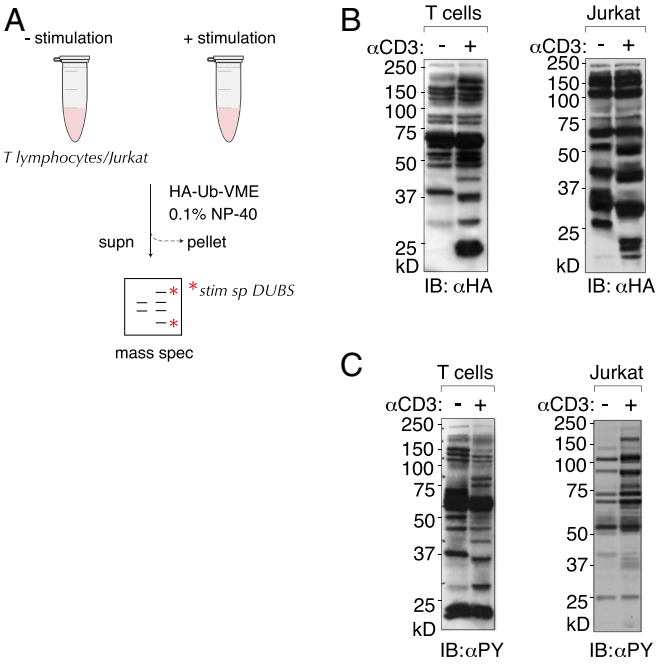


**Fig. 1.** Functional DUBs in the TCR signaling pathway can be identified using HA-Ub-VME. (*A*) Schematic of the experimental setup. Primary T cells or Jurkat cells were either mock-treated or stimulated with anti-CD3 antibody in the presence of HA-Ub-VME. HA-reactive material was immunoprecipitated and identified through mass spectroscopy. (*B*) (*Left*) 20 × 10$^6$ cells isolated from mice were split in two and either mock-treated or anti-CD3 antibody-treated in buffer containing 50 mM Tris, 5 mM $MgCl_2$, 150 mM NaCl, and protease and phosphatase inhibitors. Cells were stimulated for 20 min and lysed in 0.1% Nonidet P-40. Supernatants were resolved by SDS/PAGE and visualized by immunoblotting with anti-HA. (*Right*) 20 × 10$^6$ Jurkat cells were treated as described above. (*C*) Primary T cells (*Left*) and Jurkat cells (*Right*) from the same experiment were resolved on SDS/PAGE and visualized by immunoblotting using anti-phosphotyrosine antibody to measure the TCR signaling cascade.

either mock-treated for control or stimulated with anti-CD3. Anti-HA–conjugated beads were used to immunoprecipitate DUBs from resting and stimulated primary T cells. Immunoprecipitated material was resolved on SDS/PAGE and visualized by silver staining (Fig. 2*B*). The entire lanes for both control and stimulated samples were divided into 2-mm-thick slices and subjected to trypsin digest, followed by proteomic analyses on a high-resolution Thermo Fisher Orbitrap Elite mass spectrometer. Several enzymes of the Ub conjugation machinery, including DUBs, E2s, and some E3 ligases, were identified in the mass spectroscopy dataset (Table 1).

To validate the hits identified through mass spectroscopy, we used Jurkat cells, which are more amenable to genetic manipulation. As described above, cells were either mock- treated or stimulated with anti-CD3 in the presence of HA-Ub-VME for 20 min, and then lysed in 0.1% Nonidet P-40. Supernatants were resolved by SDS/PAGE and immunoblotted with antibodies against a subset of the hits listed in Table 1 (Fig. 2*C*). Usp12, Usp46, and OtuB1 were among the most prominent hits, with distinct peptide counts in the control and stimulated samples. Both Usp12 and 46 were modified by HA-Ub-VME and displayed enhanced recovery in stimulated samples compared with resting cells. Usp12 and Usp46 carry putative nuclear localization signals and are typically enriched in the nucleus.

Because transcription/translational regulation is unlikely to play a significant role in the time frame of 20 min of TCR stimulation, we hypothesized that the differential recovery of DUBs in the control vs. stimulated samples was due primarily to their

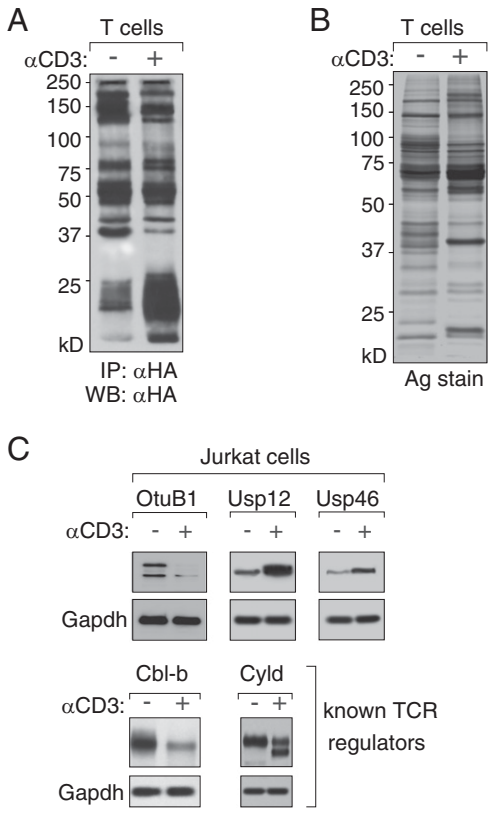


**Fig. 2.** Identification and validation of functional DUBs in the TCR signaling pathway. (*A*) Approximately $20 \times 10^6$ T cells were isolated from mice, split in two, and either mock-treated or stimulated with anti-CD3 for 20 min in the presence of 1 μM HA-Ub-VME. Cells were lysed in 0.1% Nonidet P-40. Supernatants were immunoprecipitated on conjugated anti-HA beads. Bound material was eluted by boiling in Laemmli buffer and resolved by SDS/PAGE, followed by immunoblotting with anti-HA antibodies. (*B*) Approximately $110 \times 10^6$ T cells were isolated from mice and analyzed as described above. Immunoprecipitated material was visualized by silver staining. The entire lanes for control and stimulated samples were sliced into 1-mm sections and submitted for mass spectroscopy. (*C*) Immunoblots against identified hits in mock-treated vs. stimulated samples.

redistribution from the nucleus to the cytosol. Hits that displayed a decrease in peptide counts in stimulated samples undergo either rapid degradation or relocalization to the nucleus. OtuB1 has been described to have two different isoforms with distinct half-lives, and to undergo degradation on stimulation (37, 38) (Fig. 2*C*). Similarly, Cbl-b expression levels were attenuated in stimulated samples owing to rapid turnover (39–42).

Our mass spectroscopy dataset contained several DUBs, including those that have been described previously in the context of TCR signaling, such as CYLD and Usp9X, as well as other enzymes of the ubiquitylation machinery, such as Cbl-b. The entire population of CYLD was modified by HA-Ub-VME in resting cells but migrated as a double band in stimulated samples, suggesting partial inactivation (Fig. 2*C*). Among the lead hits, we focused on Usp12 and Usp46, because they displayed a consistent increase in recovery from the stimulated samples and had not been described previously.

**Usp12 and Usp46 Translocate from the Nucleus to the Cytosol on TCR Stimulation.** Usp12 and Usp46 share nearly 90% amino acid sequence homology, and both are equipped with nuclear export signals. To measure their cellular localization on TCR stimulation, cells were either mock-treated or stimulated with anti-CD3 for 20 min. Cytosol fractions were separated from the residual subcellular organelles using perfringolysin O (PFO), a pore-forming toxin that selectively permeabilizes the plasma membrane without damaging the internal membranes, as described elsewhere (43–47). In resting cells, Usp12 and Usp46 are localized primarily to the nucleus; however, when stimulated with anti-CD3, both exhibited significant enrichment in the cytosol fractions (Fig. 3*A*). Under resting conditions, the cytosolic fraction was ∼20% of the total intracellular level for each. On TCR activation, ∼80% of the total protein for both Usp12 and Usp46 became available in the cytosol, indicating that they relocalize from the nucleus (Fig. 3*A*).

To further analyze this biochemical behavior, Jurkat cells were stimulated with anti-CD3 for various time intervals (Fig. 3*B*). Resting cells were treated in parallel. At each time point, cells were treated with PFO to separate cytosol and pellet fractions. Cell lysates in 0.1% SDS were used to measure total expression levels. Both Usp12 and Usp46 displayed a gradual appearance in the cytosol as a function of time on TCR stimulation (Fig. 3*B*). These data imply that engagement of the TCR and proximal signaling can be rapidly sensed in the nucleus to allow transport of Usp12 and Usp46 to the signalosome within 20 min of stimulation. The factors essential for this process remain unknown; however, nucleocytoplasmic transport is often facilitated through protein phosphorylation.

To measure whether Usp12 was phosphorylated on TCR stimulation, resting and activated Jurkat cells were treated with PFO to separate cytosol and nuclear fractions, treated with a phosphatase enzyme, and resolved by 15% (wt/vol) SDS/PAGE (Fig. 3*C*). In addition, Usp12 immunoprecipitated from cytosol and nuclear fractions was immunoblotted with anti-pY antibodies (Fig. 3*D*). TCR stimulation induced phosphorylation of the cytosolic pool of Usp12, as measured by phosphatase treatment as well as immunoblotting for the phosphorylated fraction of Usp12. Taken together, our data suggest the involvement of one or more kinases in the relocalization process of Usp12 and Usp46.

**Usp12-Deficient Cells Display Defective MAPK, NFκB, and NFAT Activities on TCR Stimulation.** To understand the physiological role of Usp12 and measure activities of downstream effectors of TCR signaling, we generated Jurkat cells expressing a doxycycline-inducible Cas9 nuclease to create a Usp12 knockout. After induction for 3–5 d, cell lysates were immunoblotted for Flag-Cas9 and Usp12, which confirmed expression of Cas9 and deletion of Usp12 (Fig. 4*A*). Usp12$^{-/-}$ cells exhibited no gross defects in morphology except for delayed growth kinetics.

To assess the function of Usp12 in TCR signaling, we measured total phosphorylation levels in control and Usp12$^{-/-}$ cells. Phosphotyrosine levels were significantly diminished in anti-CD3–stimulated Usp12$^{-/-}$ cells (Fig. 4*B*). Specifically, we measured the

**Table 1. Deubiquitylating enzymes retrieved by HA-Ub-VME**

| Protein | Accession no. | Molecular weight, kDa | Unique peptides | |
|---|---|---|---|---|
| | | | Mock | Stimulated |
| USP4 | 164519045 | 109 | 19 | 8 |
| USP7 | 154146209 | 113 | 23 | 7 |
| USP12 | 34328057 | 43 | 14 | 34 |
| USP24 | 260064007 | 294 | 18 | 11 |
| USP25 | 31980712 | 126 | 21 | 28 |
| UCH44 | 332205971 | 81 | 15 | 10 |
| USP46 | 29243896 | 42 | 8 | 19 |
| OTUB1 | 19527388 | 31 | 56 | 6 |
| CYLD | 189491655 | 107 | 10 | 9 |
| USP9X | 115511018 | 290 | 14 | 12 |
| USP34 | 568969979 | 460 | 10 | 6 |
| UCHL3 | 12248390 | 26 | 21 | 43 |
| UCHL5 | 229577281 | 38 | 32 | 37 |

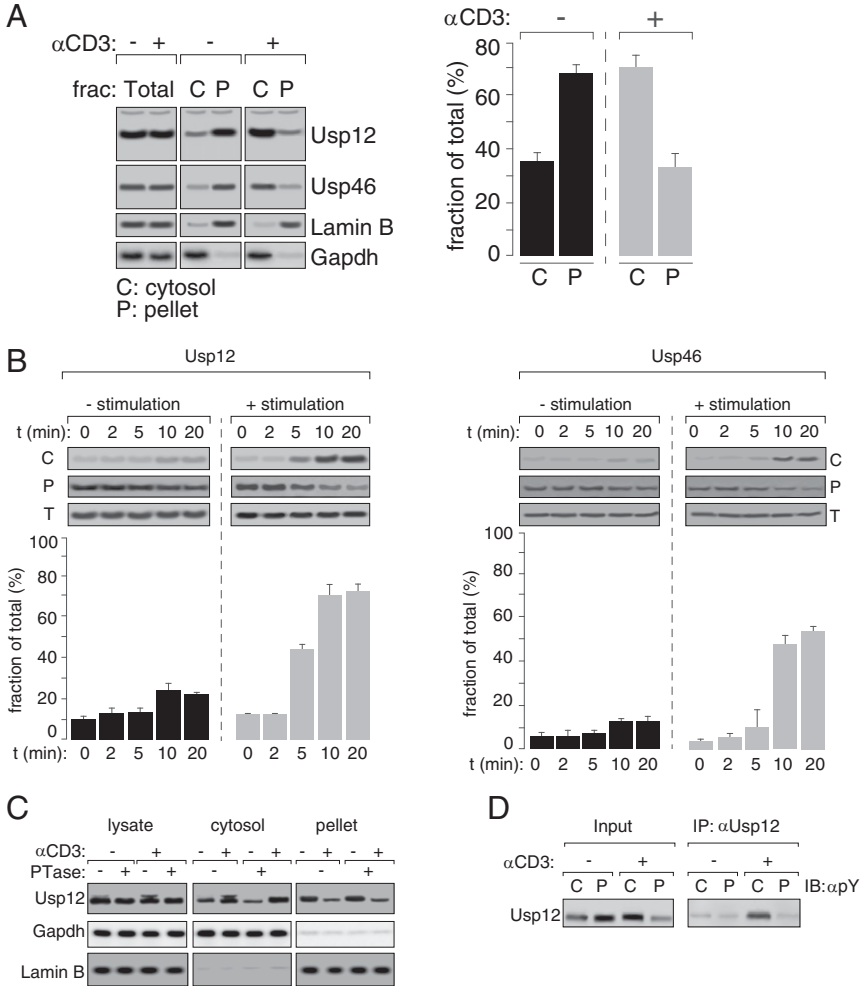


**Fig. 3.** Usp12 and Usp46 translocate from the nucleus to the cytosol on TCR stimulation. (*A*) $1 \times 10^6$ Jurkat cells were either mock-treated or stimulated with anti-CD3 antibody for 20 min. Control and stimulated cells were split in two and either permeabilized with 50 nM PFO to collect cytosol or lysed in 0.1% SDS. Cytosol fractions and total lysates were immunoblotted with antibodies against Usp12 and Usp46. Densitometric analyses were performed on immunoblots, and results are presented as the amount present in the cytosol as a fraction of the total. Images are representative of three independent experiments. (*B*) Time course of Usp12 and Usp46 translocation to the cytosol from the nucleus. Jurkat cells were stimulated for varying times and treated as described above. Unstimulated cells were processed in parallel. Densitometric analyses were performed on immunoblots. Images are representative of three independent experiments. (*C*) Resting and stimulated Jurkat cells were either lysed in 0.5% Nonidet P-40 or separated into cytosol and pellet fractions using PFO. Samples were mock-treated or subjected to shrimp phosphatase treatment for 1 h at 37 °C, resolved by SDS/PAGE, and immunoblotted for Usp12. Gapdh and Lamin B served as loading controls. (*D*) Usp12 was immunoprecipitated from either resting or stimulated cells and immunoblotted with anti-phosphotyrosine antibodies.

expression profiles of LAT, zeta, Erk1/2, and their phosphorylated forms (Fig. 4*C*). Interestingly, LAT was barely detectable on stimulation in Usp12$^{-/-}$ cells; however, CD3ζ levels remained unaffected, suggesting no impairment in formation of the proximal signaling complex. The appearance of phosphorylated Erk1/2 also was severely impaired in Usp12$^{-/-}$ cells (Fig. 4*C*, *Lower*).

To evaluate distal signaling events, we measured NFκB and NFAT activities in control and Usp12$^{-/-}$ cells. NFκB activity in these cells was measured by the appearance of phosphorylated p65 on activation. Noninduced Usp12-proficient cells served as controls. In Usp12-deficient cells, the appearance of phosphorylated p65 was significantly impaired on TCR stimulation compared with control cells (Fig. 4*D*, *Upper*).

In resting T cells, NFAT is phosphorylated and localized to the cytoplasm. Activation of T cells results in NFAT nuclear translocation, where it is dephosphorylated and initiates a specific transcriptional program. To measure Usp12-dependent NFAT activity, we immunoblotted for intracellular levels of dephosphorylated NFAT (Fig. 4*D*, *Lower*). In addition, we transfected control and Usp12$^{-/-}$ Jurkat cells with a NFAT-luciferase reporter construct and stimulated cells with varying concentrations of anti-CD3 (Fig. 4*E*). As observed for phospho-p65 of NFκB, the appearance of dephosphorylated NFAT as well as luciferase activity were inhibited in the Usp12-deficient cells (Fig. 4*E*).

Because both transcription factors displayed impaired activity, we assayed TCR expression at the cell surface in Usp12-proficient and -deficient cells. We measured the surface expression of TCR in intact cells by flow cytometry in control and Usp12$^{-/-}$ cells in resting and on stimulation. In Usp12$^{-/-}$ cells, TCR expression at the cell surface remained unaffected under resting conditions, but was significantly down-regulated on stimulation relative to controls (Fig. 4*F*, *Upper*). Total levels of TCR remained unaffected, suggesting that TCR is rapidly internalized but not degraded in Usp12$^{-/-}$ cells (Fig. 4*F*, *Lower*).

Because no compensatory effect was observed from Usp46 in Usp12-deficient cells, we measured Usp46 expression levels in the knockout cells. Surprisingly, Usp46 levels were diminished in these cells, presumably owing to degradation, suggesting that they need to form a complex to function (Fig. S1*C*).

**TCR Activity Is Rescued in Usp12-Reconstituted Cells.** To rescue the function of Usp12, we reconstituted a wild type (WT) HA-Usp12 in a Usp12$^{-/-}$ background. HA-Usp12 was expressed in knockout Jurkat cells by electroporation (Fig. 5*A*). The subcellular distribution of ectopic HA-Usp12 in resting and stimulated cells resembled the distribution of endogenous Usp12 (Fig. 5*B*). We measured the functional rescue of TCR signaling in WT, Usp12$^{-/-}$, and Usp12 reconstituted cells in three distinct ways: (*i*) phosphorylation profiles on TCR stimulation, (*ii*) NFAT and NFκB activities, and (*iii*) expression levels of the TCR and its adaptors. Control and Usp12 reconstituted cells were stimulated with anti-CD3, and lysates were probed with anti-pY. Bulk phosphorylation profiles, as well as the appearance of pErk1/2 in Usp12 reconstituted cells, closely resembled those in WT cells (Fig. 5*C*). NFκB and NFAT activities, as measured by the appearance of

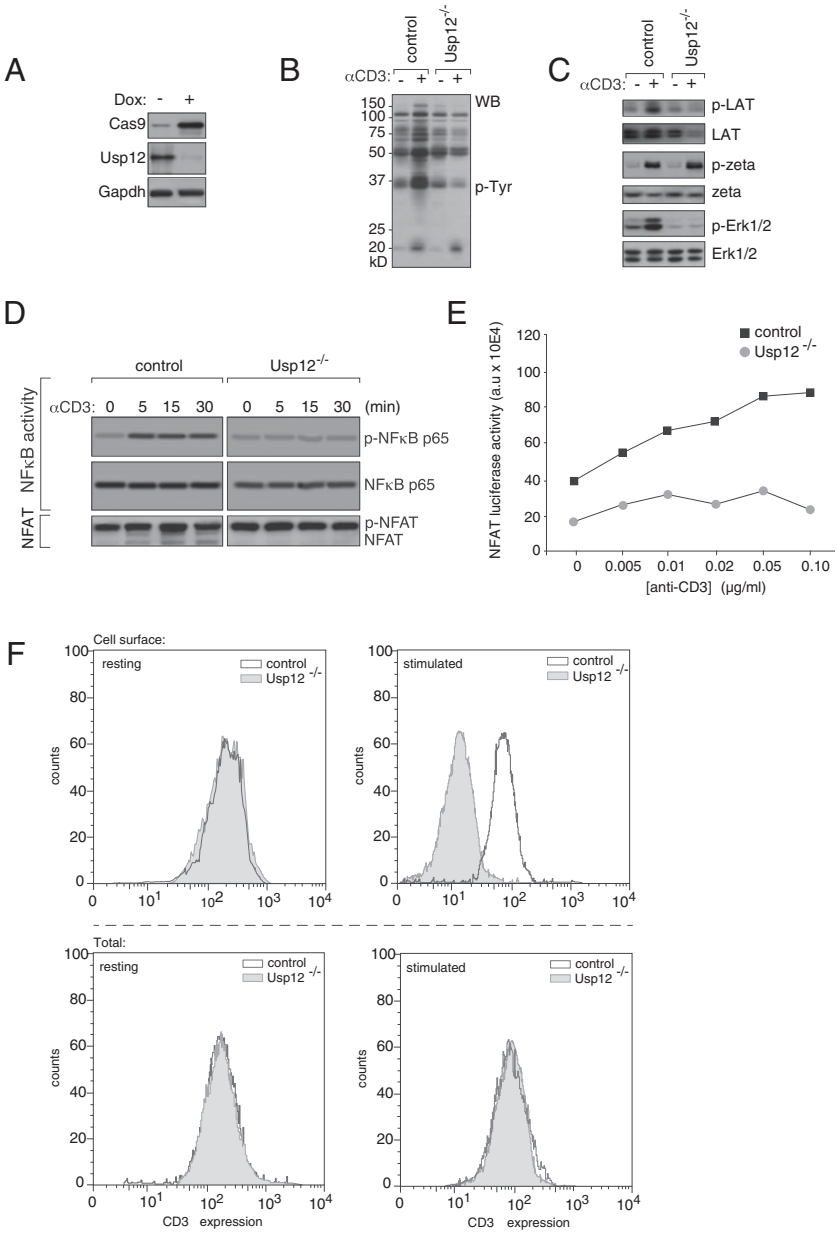


**Fig. 4.** Cas9/CRISPR mediates knockout of Usp12 in Jurkat cells. (*A*) Jurkat cells stably expressing doxycycline-inducible Cas9 were transduced with gRNA targeting Usp12, cloned into a lentiviral expression vector, and selected on hygromycin. After doxycycline induction for 3–7 d, cells were lysed and then immublotted to verify deletion of Usp12. (*B* and *C*) WT and Usp12$^{-/-}$ knockout Jurkat cells were stimulated with anti-CD3 for 20 min, after which TCR signaling was visualized using anti-phosphotyrosine or antibodies against LAT, pLAT, CD3ζ, pCD3ζ, p-Erk1/2, and Erk1/2. (*D*) Lysates were collected from control and Usp12$^{-/-}$ Jurkat cells that were either mock-treated or stimulated with anti-CD3. NFκB and NFAT activities were measured by immunoblotting for the phosphor-NFκB p65 subunit and pNFAT. (*E*) Control and Usp12$^{-/-}$ Jurkat cells were electroporated with a dual luciferase reporter construct to measure NFAT activity. Cells were either mock-treated or stimulated with anti-CD3, and a luciferase assay was performed in accordance with the manufacturer's protocol. (*F*) WT and Usp12$^{-/-}$ knockout cells were either at rest or simulated with anti-CD3 for 20 min, fixed, and stained with PE-conjugated anti-CD3 in intact cells for surface expression or in permeabilized cells for total levels.

phosphorylated p65 and luciferase reporter assay, respectively, were significantly rescued in cells expressing Usp12 (Fig. 5*D*). In addition, surface expression of TCR in HA-Usp12 reconstituted cells was restored to WT levels (Fig. 5*E*). These data support the idea that the phenotypic defects in Usp12$^{-/-}$ cells are specific and dependent on Usp12 activity.

To establish a functional relevance of the cytosolic pool of Usp12, we reconstituted Jurkat cells with a Usp12 variant mutated in its nuclear export signal (NES) or treated Jurkat cells with leptomycin B to prevent transport of the nuclear localized fraction to the cytosol (Fig. 5*F* and Fig. S2). We separated these cells into cytosol and nuclear fractions using PFO to measure the distribution of Usp12 on stimulation. With a mutated NES, Usp12 remained localized to the nucleus in both resting and stimulated cells (Fig. 5*F*). Surface expression of TCR was diminished on stimulation with anti-CD3, confirming the requirement of Usp12 activity in the cytosol. As with NES-defective Usp12, leptomycin treatment resulted in reduced TCR surface expression on anti-CD3 stimulation (Fig. S2).

**Identification of Usp12 Substrates in the TCR Signaling Pathway.** We identified possible substrates of Usp12 with the recently developed proximity- dependent protein labeling technique using a modified biotin ligase (48, 49). We expressed Usp12 fused to BirA-ligase in Jurkat cells cultured in medium supplemented with biotin. Vicinal proteins as well as transient interactors are biotinylated by the ligase and can be affinity-captured on streptavidin beads. Cells were either mock-treated or stimulated with anti-CD3 antibodies and subjected to immunoprecipitation. Copurifying proteins were resolved by SDS/PAGE, visualized by Coomassie blue staining, and identified using mass spectroscopy (Fig. 6*A*). Not surprisingly, a large number of proteins were recovered using the BirA-Usp12 (BioID) approach, because transient interactors are effectively captured by this strategy. The Usp12 interactomes obtained in activated T cells were distinct from those in resting cells, as seen on the Coomassie blue-stained protein profiles. Prominent interactors included Usp46, ITCH, Wdr48, Wdr20, Trat1, Lat, SLP-76, Grb2, and Cbl-b, most of which were verified by immunoblotting (Fig. 6*B*). Interestingly, Usp46, Wdr20, and Wdr48 were recovered

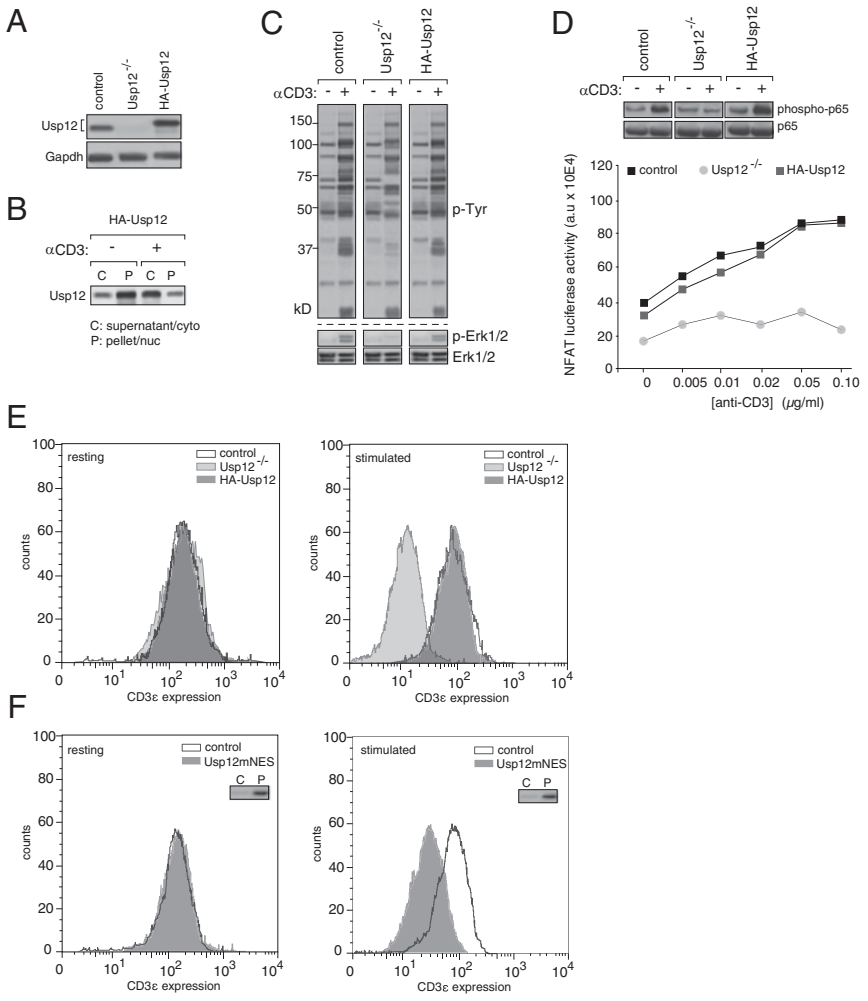


**Fig. 5.** TCR function is rescued in Usp12$^{-/-}$ cells reconstituted with HA-Usp12. (*A*) Stable expression of HA-Usp12 in Usp12$^{-/-}$ cells was verified using anti-Usp12 antibodies. (*B*) $1 \times 10^6$ Jurkat cells expressing HA-Usp12 were either mock-treated or stimulated with anti-CD3 antibody for 20 min. Control and stimulated cells were permeabilized with 50 nM PFO to separate cytosol and nuclear fractions and then immunoblotted for Usp12. (*C*) TCR signaling in control, Usp12$^{-/-}$, and HA-Usp12–expressing cells was visualized by anti-pY antibodies (*Upper*) and anti-pErk1/2 (*Lower*). (*D*) NFκB activity was measured by immunoblotting for the phosphor-NFκB p65 subunit (*Upper*) and by a luciferase reporter assay for NFAT activity (*Lower*). (*E*) WT, Usp12$^{-/-}$, and HA-Usp12–expressing Jurkat cells were either mock-treated or simulated with anti-CD3 for 20 min, fixed, and stained with PE-conjugated anti-CD3. (*F*) WT and HA-Usp12mNES–expressing Jurkat cells were either mock-treated or simulated with anti-CD3 for 20 min, fixed, and stained with PE-conjugated anti-CD3.

as interactors from both resting and stimulated cells, indicating that they might function as a complex in both the nucleus and the cytosol. However, given the lack of functional redundancy of Usp46 and Usp12, it is possible that different cofactors play a role in determining their function.

Among the prominent hits were several adaptors of the TCR that have been previously reported to stabilize the TCR complex at the cell surface. We measured the expression of these candidate proteins in control and Usp12$^{-/-}$ cells at rest and on stimulation by FACS staining and immunoblotting (Fig. 6 *C* and *D*). We measured the expression of Class- I and CD45 as controls in parallel. Usp12-deficient cells exhibited attenuated expression of both LAT and Trat1, presumably owing to their degradation; however, SLP-76 expression remained unchanged under identical conditions. Expression levels of Class-I and CD45 were unaffected, as anticipated. These results suggest that on TCR activation, LAT and Trat1 are ubiquitylated and degraded in the absence of Usp12.

To confirm whether LAT and Trat1 are substrates of Usp12, we immunoprecipitated these proteins from control and Usp12$^{-/-}$ cells transfected with HA-Ub, treated with either chloroquine or MG132 to inhibit lysosomal and proteasomal activities, respectively (Fig. 6 *E* and *F*). We added purified EBV-DUB—a promiscuous DUB—as a means of removing any Ub modifications on substrates (50). Both LAT and Trat1 were seen to undergo monoubiquitylation in a Usp12-dependent manner (Fig. 6*E*). Interestingly, a fraction of Ub-modified LAT was recovered in Usp12$^{-/-}$ cells even without lysosomal inhibition. A minor fraction of polyubiquitylated Trat1 and LAT was captured on proteasomal inhibition with MG132 (Fig. 6*F*); however, given that the abundance of this fraction remained unaffected in WT and Usp12$^{-/-}$ cells, this phenomenon appears to occur independently of Usp12 and has been reported previously (51). Our results support LAT and Trat1 as bona fide substrates that undergo monoubiquitin modification and lysosomal degradation in the absence of Usp12.

## Discussion

The importance of Ub and Ub-like small modifiers in regulating signal transduction pathways has been extensively documented (52–54). Among the repertoire of such modifiers, Ub has received the most attention. Major advances have been made in understanding its role in cellular degradation processes; however, its function in protein activation and subcellular localization is far less well understood. Gaining deeper insight into the functional outcomes of different linkage specificities has proven far more technically challenging (35, 36, 55).

The activation of the TCR on encountering an antigen engages an extensive array of proteins for recruitment of downstream effectors, culminating in nuclear translocation of transcription factors such as NFκB and NFAT (56). Regulation of such a vast number of proteins is stringently executed by a number of post-translational modifications (PTMs), including phosphorylation, ubiquitylation, and other small-molecule modifiers. The reversibility of ubiquitylation and phosphorylation provided by the corresponding DUBs and phosphatases allows fine-tuning of the duration and magnitude of signaling cascades. Various deubiquitylating enzymes that function in the TCR signaling pathway, including CYLD,

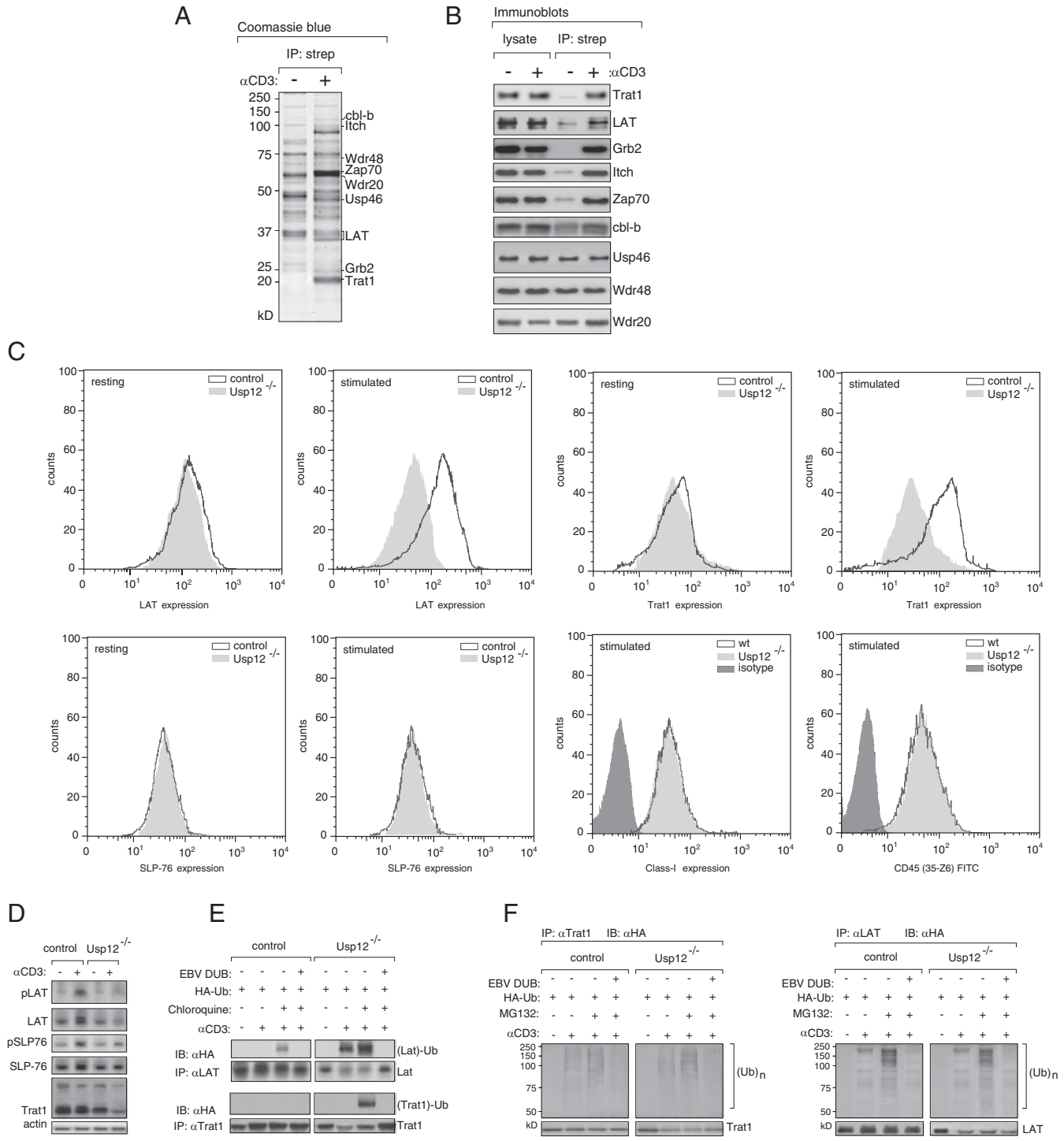


**Fig. 6.** Functional characterization of Usp12 in the TCR signaling pathway. (*A*) BirA ligase was fused at its C terminus to Usp12, expressed in Jurkat cells, and cultured in medium supplemented with biotin. Control and anti-CD3–stimulated cells were lysed in 0.5% Nonidet P-40 and immunoprecipitated on streptavidin beads. Eluted material was resolved by SDS/PAGE and visualized by silver staining. Prominent bands were subjected to analyses by mass spectroscopy. (*B*) Lysates and immunoprecipitated material from the procedure shown in *A* were immunoblotted with antibodies against Lat, Trat1, Grb2, Itch, Cbl-b, Wdr20, Wdr48, and Usp46 to confirm the mass spectroscopy hits. (*C*) Expression of LAT and Trat1 (*Upper*) and of SLP-76, Class-I, and CD-45 (*Lower*) at rest and on stimulation in control and Usp12$^{-/-}$ cells as analyzed by FACS. (*D*) Immunoblots against pLAT, LAT, Trat1, pSLP-76, and SLP-76 in control and Usp12$^{-/-}$ cells. (*E*) LAT and Trat1 were immunoprecipitated from WT and Usp12$^{-/-}$ cells expressing HA-Ub and stimulated with anti-CD3. Immunoprecipitation was performed from cells either mock-treated or chloroquine-treated to inhibit lysosomal degradation and immunoblotted with anti-HA antibodies. (*F*) Immunoprecipitation was performed as in *E*, with MG132 treatment to block proteasomal degradation.

USP9X, and A20, have been described previously (6, 28, 35, 55, 56). Additional siRNA screens for DUBs in TCR function have identified Usp34 as a negative regulator of the process (57).

In contrast to genetic screening approaches, a chemical proteomics strategy avoids previous genome modification and associated off-target effects while providing the advantage of

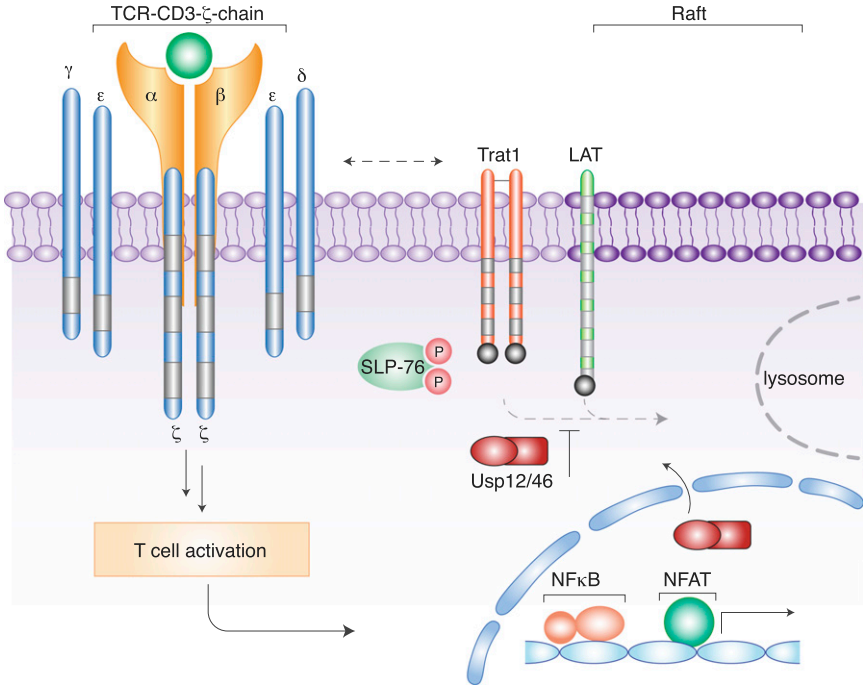


**Fig. 7.** Proposed model for Usp12 function in the pathway of TCR signaling. A model for Usp12 function in TCR activation is illustrated. Following TCR engagement, protein tyrosine kinases are activated, resulting in phosphorylation of CD3 modules and further activation of downstream kinases and phosphorylation events. Phosphorylated LAT and SLP-76 associate with other adaptors, such as Trat1, Grb2, and PLCγ, resulting in formation of a multimeric complex. TCR and adaptor molecules, such as LAT, Trat1, and SLP-76, are constitutively monoubiquitylated to undergo internalization and recycling or degradation from the lysosomes. During TCR engagement and activation, Usp12 is translocated into the cytosol and deubiquitylates its substrates to stabilize the TCR signaling complex at the plasma membrane. In the absence of Usp12, formation of the multimeric complex at the plasma membrane is significantly diminished owing to reduced expression of adaptor molecules as well as the TCR, resulting in inhibition of NFκB and NFAT.

investigating signaling in primary T cells. Furthermore, the use of activity-based probes offers the possibility of capturing enzymatic changes occurring in the time frame of TCR signaling. We identified known regulators of TCR signaling, including OTUB1 (37, 38), CYLD (31, 57), USP9X (32), and USP34 (57), validating our approach while identifying potential new players (Table 1). We show that Usp12 and Usp46 are both constitutively expressed in T cells, where they are localized predominantly in the nucleus, as previously reported by others in cell lines (58, 59). Usp12 and Usp46 have been shown to deubiquitylate histone 2A and 2B through a process requiring interaction with Wdr48 (58). The retrieval of Wdr48 following immunoprecipitation from stimulated T cells suggests that a similar complex might be required for enzymatic activity in the cytoplasm. Our results demonstrate that Usp12 and Usp46 are rapidly redistributed to the cytosol with similar kinetics on TCR engagement, possibly as part of the same molecular complex, as suggested by proximity-dependent labeling experiments.

The stimulation-dependent phosphorylation of Usp12 may induce its translocation and/or activation. Our experiments in Usp12-deficient and reconstituted Jurkat cells clearly demonstrate that early events in TCR signaling, such as phosphorylation of CD3ζ, do not require Usp12. In marked contrast, phosphorylation of LAT was defective in the absence of Usp12, affecting most of the distal signaling (MAPK, NFκB, and NFAT). Because Usp12 deficiency resulted in a drastic decrease in the surface-exposed fraction of the TCR complex on stimulation, as well as in the expression levels of LAT and Trat1 (Fig. 6*A*), we hypothesized that translocation of Usp12 to the cytoplasm is required for stabilization of the proximal signaling hub as shown (Fig. 7). Mono-Ub modification and lysosomal degradation of LAT and Trat1 in Usp12$^{-/-}$ cells strongly support our hypothesis.

A number of studies have been performed to evaluate the stability, internalization, and recycling of the TCR in naïve and stimulated cells. Available evidence supports that the TCR is internalized and recycled quite rapidly (12, 21). The constitutive endocytic rate constant in resting T cells is ∼0.01min$^{-1}$; however, the fraction recycled vs. the fraction degraded has not been resolved. Our results suggest that on stimulation, Usp12 is recruited to stabilize the TCR at the plasma membrane for the amplitude to reach a threshold so as to turn on NFκB-responsive genes. These data are in line with previous reports on LAT and Trat1, which appear to regulate expression of the TCR at the cell surface (15, 60). Hyperubiquitylation of LAT has been found to reduce TCR levels at the cell surface (51), whereas overexpression of Trat1 stabilizes TCR levels (60). The phenotypic effect of Usp12 deletion appears to be similar; on stimulation of T cells, LAT and Trat1 expression is significantly reduced in Usp12$^{-/-}$ cells. Interestingly, despite the close sequence homology and similar biochemical characteristics, Usp46 does not compensate for a deletion in Usp12, as also has been reported for histone ubiquitylation (58). Such specificity might be conferred by adaptor proteins such as Wdr48 and Wdr20, which function as part of the complex. In line with our in vitro findings, Usp12$^{-/-}$ mice have been found to have significantly fewer CD8$^{+}$ T cells (as annotated by the International Mouse Phenotyping Consortium database), underscoring Usp12's role in T-cell development.

Usp12 removes Ub modifications placed by an E3 ligase, whose activity is presumably regulated by TCR signaling. Interestingly, among the E3 ligases retrieved as interactors of Usp12 through proximity-based labeling, we isolated both Cbl-b and Itch. GRAIL, another E3-ligase, has been shown to ubiquitylate CD3ζ (61). Both GRAIL deficiency and Cbl-b deficiency induce TCR stabilization as well as enhanced T-cell responses (40, 41, 61). Whether Usp12 counteracts the activity of GRAIL, Cbl-b, Itch, or any other E3 ligase remains to be determined. Nevertheless, given its upstream position in the signaling cascade, we predict that the

expression, translocation, or activity of Usp12 (and its cointeractors) will be differentially regulated in naïve, effector, anergic, or regulatory T cells for the purpose of cell function. Indeed, it has been demonstrated that whereas GRAIL deficiency enhances effector T-cell function, it decreases regulatory T cells' suppressive capacity (61), arguing for a subset-specific regulation of TCR complex stability.

The present study describes an unbiased activity-based approach to investigating posttranslational modifications that follow TCR engagement. Its simplicity lends itself to the study of signaling pathways downstream of antigen-specific or pattern-recognition receptors. Uncovering posttranslational modifiers in immune pathways not only extends our understanding of signaling events, but also provides new targets suitable for therapeutic intervention.

## Experimental Procedures

**Plasmids, Antibodies, Cell Lines, and Constructs.** Jurkat cells (E6.1) were purchased from American Type Culture Collection and maintained in RPMI supplemented with 10% FCS, 1% penicillin-streptomycin, and 2% glutamine at 37 °C. BirA*-ligase cloned into pcDNA3.1 was obtained from Addgene. The Myc-BirA* module was amplified from the pcDNA3.1(–) cloning vector with the incorporation of additional restriction enzyme sites by PCR. The module was ligated into the pLJM1 expression vector between the HindIII and BamHI sites to generate the new pLJM1_Myc_BirA* plasmid. The complete Usp12 ORF was subcloned into the vector between the XhoI and AflII sites. Plasmid encoding PFO was provided by Art Johnson (Texas A&M University).

Mouse mAbs used included anti-phosphotyrosine (4G10; Santa Cruz Biotechnology and the BD Transduction laboratory), anti-Trat1 (clone Trim-04, PE-conjugated; Novus Biologicals), and anti-ZAP-70 (2F3.2), anti-LAT (2E9), anti-NFκB p65, and anti–phospho-NFκB p65 (Abcam and Cell Signaling Technology). Antibody against the HA epitope was purchased from Roche (3F-10). Antibodies against Usp12, Usp46, OtuB1, and Cbl-b were purchased from Abcam. Purification and optimization of PFO have been described previously (44). HA-agarose beads were purchased from Roche Applied Science, and protein A-agarose beads were obtained from RepliGen Bioprocessing.

**Assay with HA-Ub-VME to Capture DUBs.** Approximately $20 \times 10^6$ T-cells were isolated from WT mice and split into two groups. Cells were stimulated with anti-CD3 in a reaction volume of 100 μL of buffer (Tris·HCl pH 7.5, 150 mM NaCl, and 5 mM $MgCl_2$) containing 10 μM HA-Ub-VME supplemented with phosphatase and protease inhibitors. Control cells were treated in parallel without antibody. Stimulation with anti-CD3 was performed for 20 min at 37 °C, followed by lysis in buffer containing 0.1% Nonidet P-40 for 30 min on ice. Supernatants were separated from the nuclear material and unbroken membranes by a brief centrifugation, boiled for 5 min in Laemmli buffer, and resolved by SDS/PAGE. HA-reactive material was visualized by immunoblotting with HRP-conjugated anti-HA antibodies.

**Designing the CRISPR Target Sequence and Prediction of Off-Target Effects.** The target sequence preceding the PAM motif was obtained from the region of the exon of Usp12. The following sequences were used for generating gRNA sequences for the two variants of Usp12: hUSP12-Cr1, cggtcaatgagcactattt; hUSP12-Cr2, tcttgtgatgaacttctta. Potential off-target effects of the target sequence were confirmed using the National Center for Biotechnology Information's *Homo sapiens* Nucleotide BLAST.

**Generation of the CRISPR RNA Lentivirus Vector.** CRISPR gBlock was designed to incorporate into the restriction enzymatic site NheI/BamHI of CMV promoter-deleted pCDH-EF1-Hygro as follows. The gBlock was digested by NheI and BamHI restriction enzymes, then incorporated into the pCDH vector linearized with the same restriction enzyme. Genotyping of the CRISPR-Cas9–mediated knockout cells using the SURVEYOR assay was performed as described previously (62).

**Generation of Jurkat Cells Expressing Inducible Cas9-3X-Flag.** Jurkat cells were seeded in 10-cm dishes at a density of $4 \times 10^6$ along with 30 μL of concentrated virus and incubated at 37 °C overnight, followed by the addition of fresh medium. At 48 h postinfection, culture medium supplemented with 0.5 μg/mL puromycin was added. Selection pressure was maintained for 2 wk with medium changes every 2 d. For expression of Cas9, cells were induced with 1 μg/mL of doxycycline for 3–7 d and then immunoblotted with anti-Flag antibodies. For Usp12 knockout, Jurkat cells expressing inducible Cas9 were seeded at a density of $4 \times 10^6$ along with 30 μL of concentrated lentivirus generated for gRNAs. Cells were selected with 1 mg/mL hygromycin for 2 wk. Knockout of Usp12 was measured after induction of Cas9 for 3–7 d, followed by immunoblotting in uninduced and Cas9-expressing cells.

**Cytosol Fractionation Using PFO.** For separating cytosol fractions, $\sim 1 \times 10^7$ cells were washed once and resuspended in 50 μL of PBS on ice. Then 50 μL of 200 nM PFO was added to cells in suspension to obtain a final concentration of 100 nM, which was maintained on ice for 5 min. Excess PFO (i.e., unbound to the plasma membrane) was removed by diluting with 1 mL of PBS and centrifugation at $500 \times g$ for 5 min. Cell pellets were resuspended in 50 μL of HBSS and incubated at 37 °C for 10 min.

Following permeabilization, cells were centrifuged at $500 \times g$ for 5 min to collect supernatants. Pellets thus obtained were washed once with 1 mL of PBS and resuspended in 50 μL of PBS containing 0.5% Nonidet P-40. Both cytosol and pellet fractions were resolved by SDS/PAGE and subjected to immunoblotting for Usp12 and Usp46.

**Phosphatase Assay.** WT Jurkat cells ($5 \times 10^6$ per condition) were either mock-treated or stimulated with anti-CD3 for 20 min at 37 °C. Cells were lysed in 200 μL of either (*i*) 50 mM Tris·HCl, 150 mM NaCl, 5 mM $MgCl_2$, and 0.5% Nonidet P-40, with vortexing for complete lysis, or (*ii*) 100 nM PFO as described above to separate cytosol and pellet fractions. For phosphatase treatment, 5 U of shrimp alkaline phosphatase (Affymetrix) was added to 200 μL of reaction volume, incubated at 37 °C for 1 h, and then heat-inactivated at 65 °C. Samples were resolved by SDS/PAGE and visualized by immunoblotting.

**NFκB Activity in WT and Usp12$^{-/-}$ Cells.** WT and Usp12$^{-/-}$ Jurkat cells were stimulated with anti-CD3 for the indicated times. At each time point, cell pellets were collected by centrifugation at $500 \times g$ for 5 min at 4 °C. Expression of phosphorylated NFκB p65 was measured by lysing $\sim 5 \times 10^6$ Jurkat cells in 500 μL of buffer containing 50 mM Tris pH 7.5, 150 mM NaCl, 5 mM $MgCl_2$, 0.5% Nonidet P-40, and 0.1% SDS for 30 min on ice, mixed with sample buffer, and resolved by SDS/PAGE. NFκB activity was measured by immunoblotting for NFκB and the phosphorylated NFκB p65 subunit.

**ELISA and Luciferase Assays.** For ELISA, Usp12$^{-/-}$ Jurkat cells were stimulated with plate-bound CD3 mAb UCHT-1. All stimulations were done in triplicate and carried out in RPMI supplemented with 10% FCS at 37 °C for 24 h. ELISA was performed from culture supernatants following the manufacturer's instructions.

For the NFAT luciferase assay, a firefly luciferase construct downstream of the NFAT-responsive element was cotransfected with *Renilla* luciferase pLR-TK plasmid (Promega) into WT and Usp12$^{-/-}$ Jurkat cells through electroporation. Cells were stimulated with anti-CD3 for 20 min at increasing antibody concentrations, and luciferase activity was measured with light emission using the Promega Dual Luciferase Kit, with firefly luminescence units normalized to *Renilla* firefly luciferase luminescence units.

**Leptomycin B Treatment.** Jurkat cells were treated with 25 ng/mL leptomycin B for 2 h at 37 °C, followed by stimulation for 20 min with anti-CD3. Cells were then either lysed in 0.5% Nonidet P-40 to measure phosphortyrosine and phosphor-Erk1/2 or fractionated into cytosol and pellet fractions to measure the distribution of Usp12. Surface expression of TCR was measured with PE-labeled mAb UCHT-1 in fixed intact cells using flow cytometry.

**Flow Cytometry for Expression of TCR Adaptors.** Jurkat T cells expressing inducible Cas9-3X-Flag and gRNA targeting Usp12 were either mock-treated or treated with 1 μg/mL doxycycline. Following 3–7 d of induction, $1 \times 10^6$ cells from each were washed with PBS. For surface expression of TCR, cells were fixed and incubated on ice with 5 μL of PE-labeled mAb UCHT-1 for 30 min in cold PBS supplemented with 0.1% BSA. Unbound antibodies were washed, and labeled cells were resuspended in medium at 37 °C for 30 min. Negative controls of cells either not stained with antibody or stained with an isotype control were processed in parallel. The reaction was terminated with cold buffer containing 0.1% $NaN_3$, followed by centrifugation to pellet the cells, washing, and analysis by flow cytometry. For intracellular staining, cells were fixed with 0.01% formaldehyde and permeabilized with 0.5% saponin in PBS before staining with anti-LAT, anti-Trat1, W6-32 (Class-I), or anti-CD45.

**BioID and Affinity Capture of Usp12 Interactors.** Approximately $10^7$ Jurkat cells expressing BirA-Usp12 were cultured in medium supplemented with 1 μg/mL doxycycline and 50 μM biotin. Cells were lysed in 1 mL of lysis buffer [50 mM Tris pH 7.5, 150 mM NaCl, 5 mM EDTA, 1 mM DTT, 0.5% TX-100, 0.1% SDS, and 1× cOmplete Protease Inhibitor (Roche)]. Lysates were incubated with 500 μL of Neutravidin beads with end-over-end rotation for 3 h at 4 °C. Bound material

was washed with buffer containing 0.5% TX-100 and eluted in 50 μL of Laemmli buffer saturated with biotin. One-tenth of the sample was reserved for Western blot analyses. Samples reserved for analyses by mass spectroscopy were washed with 50 mM $NH_4HCO_3$ before being subjected to protease digestion.

**Treatment with Inhibitors and Immunoprecipitation.** To block proteasomal or lysosomal degradation, WT and Usp12$^{-/-}$ Jurkat cells expressing HA-Ub were treated with 5 μM MG132 and 10 μM chloroquine, respectively, for 24 h. Cells stimulated with anti-CD3 were lysed in buffer containing 0.5% Nonidet P-40, followed by immunoprecipitation on anti-LAT and anti-Trat1 antibodies. Eluted material was resolved by SDS/PAGE and immunoblotted with anti-HA antibodies to visualize Ub modification.

In leptomycin B-treated cells, Usp12 remained localized to the nucleus both at rest and on stimulation (Fig. S2*A*). Cells were lysed in 0.5% Nonidet P-40 to measure phosphortyrosine and phosphor-Erk1/2 activities. As observed for Usp12$^{-/-}$ cells, on leptomycin treatment, tyrosine as well as Erk1/2 phosphorylation was diminished relative to control cells (Fig. S2*B*). In addition, surface expression of TCR was attenuated on stimulation in leptomycin B-treated cells (Fig. S2*C*).

**ACKNOWLEDGMENTS.** We thank Takeshi Maruyama for helpful discussions. This work was funded by Institut Pasteur international network funds, an Area of Excellence Scheme of the University Grants Committee (Grant AoE/M-12/05), the Hong Kong Research Grants Council (General Research Fund Grant 17117914, to S.S.), and Health and Medical Research Fund Grant 14131102 (to S.S.).

1. Chen ZJ (2005) Ubiquitin signalling in the NF-kappaB pathway. *Nat Cell Biol* 7(8): 758–765.
2. Inn K-S, et al. (2011) Linear ubiquitin assembly complex negatively regulates RIG-I- and TRIM25-mediated type I interferon induction. *Mol Cell* 41(3):354–365.
3. Latz E, Xiao TS, Stutz A (2013) Activation and regulation of the inflammasomes. *Nat Rev Immunol* 13(6):397–411.
4. Skaug B, Chen ZJ (2010) Emerging role of ISG15 in antiviral immunity. *Cell* 143(2): 187–190.
5. Zeng W, et al. (2010) Reconstitution of the RIG-I pathway reveals a signaling role of unanchored polyubiquitin chains in innate immunity. *Cell* 141(2):315–330.
6. Düwel M, et al. (2009) A20 negatively regulates T cell receptor signaling to NF-kappaB by cleaving Malt1 ubiquitin chains. *J Immunol* 182(12):7718–7728.
7. Oeckinghaus A, et al. (2007) Malt1 ubiquitination triggers NF-kappaB signaling upon T-cell activation. *EMBO J* 26(22):4634–4645.
8. Setsuie R, Sakurai M, Sakaguchi Y, Wada K (2009) Ubiquitin dimers control the hydrolase activity of UCH-L3. *Neurochem Int* 54(5-6):314–321.
9. Guo H, et al. (2012) E3 ubiquitin ligase Cbl-b regulates Pten via Nedd4 in T cells independently of its ubiquitin ligase activity. *Cell Reports* 1(5):472–482.
10. Yang B, et al. (2008) Nedd4 augments the adaptive immune response by promoting ubiquitin-mediated degradation of Cbl-b in activated T cells. *Nat Immunol* 9(12):1356–1363.
11. Chakraborty AK, Weiss A (2014) Insights into the initiation of TCR signaling. *Nat Immunol* 15(9):798–807.
12. Favier B, Burroughs NJ, Wedderburn L, Valitutti S (2001) TCR dynamics on the surface of living T cells. *Int Immunol* 13(12):1525–1532.
13. Janes PW, Ley SC, Magee AI, Kabouridis PS (2000) The role of lipid rafts in T cell antigen receptor (TCR) signalling. *Semin Immunol* 12(1):23–34.
14. Lillemeier BF, et al. (2010) TCR and Lat are expressed on separate protein islands on T cell membranes and concatenate during activation. *Nat Immunol* 11(1):90–96.
15. Zhang W, Sloan-Lancaster J, Kitchen J, Trible RP, Samelson LE (1998) LAT: The ZAP-70 tyrosine kinase substrate that links T cell receptor to cellular activation. *Cell* 92(1):83–92.
16. Dustin ML, Depoil D (2011) New insights into the T cell synapse from single molecule techniques. *Nat Rev Immunol* 11(10):672–684.
17. James JR, et al. (2007) Single-molecule level analysis of the subunit composition of the T cell receptor on live T cells. *Proc Natl Acad Sci USA* 104(45):17662–17667.
18. Sherman E, Barr V, Samelson LE (2013) Super-resolution characterization of TCR-dependent signaling clusters. *Immunol Rev* 251(1):21–35.
19. Nijman SMB, et al. (2005) A genomic and functional inventory of deubiquitinating enzymes. *Cell* 123(5):773–786.
20. Welteke V, et al. (2009) COP9 signalosome controls the Carma1-Bcl10-Malt1 complex upon T-cell stimulation. *EMBO Rep* 10(6):642–648.
21. Liu H, Rhodes M, Wiest DL, Vignali DA (2000) On the dynamics of TCR:CD3 complex cell surface expression and downmodulation. *Immunity* 13(5):665–675.
22. Wang H, et al. (2010) Tonic ubiquitylation controls T-cell receptor:CD3 complex expression during T-cell development. *EMBO J* 29(7):1285–1298.
23. Dobrowolski R, De Robertis EM (2012) Endocytic control of growth factor signalling: Multivesicular bodies as signalling organelles. *Nat Rev Mol Cell Biol* 13(1):53–60.
24. Neefjes JJ, Hengeveld T, Tol O, Ploegh HL (1990) Intracellular interactions of transferrin and its receptor during biosynthesis. *J Cell Biol* 111(4):1383–1392.
25. Neefjes JJ, et al. (1988) Recycling glycoproteins do not return to the cis-Golgi. *J Cell Biol* 107(1):79–87.
26. Jang I-K, Gu H (2003) Negative regulation of TCR signaling and T-cell activation by selective protein degradation. *Curr Opin Immunol* 15(3):315–320.
27. Zhang Z-R, Bonifacino JS, Hegde RS (2013) Deubiquitinases sharpen substrate discrimination during membrane protein degradation from the ER. *Cell* 154(3):609–622.
28. Park Y, Jin H-S, Liu Y-C (2013) Regulation of T cell function by the ubiquitin-specific protease USP9X via modulating the Carma1-Bcl10-Malt1 complex. *Proc Natl Acad Sci USA* 110(23):9433–9438.
29. Sun L, Deng L, Ea C-K, Xia Z-P, Chen ZJ (2004) The TRAF6 ubiquitin ligase and TAK1 kinase mediate IKK activation by BCL10 and MALT1 in T lymphocytes. *Mol Cell* 14(3): 289–301.
30. Chiang YJ, et al. (2000) Cbl-b regulates the CD28 dependence of T-cell activation. *Nature* 403(6766):216–220.
31. Trompouki E, et al. (2003) CYLD is a deubiquitinating enzyme that negatively regulates NF-kappaB activation by TNFR family members. *Nature* 424(6950):793–796.
32. Naik E, et al. (2014) Regulation of proximal T cell receptor signaling and tolerance induction by deubiquitinase Usp9X. *J Exp Med* 211(10):1947–1955.
33. Schwickart M, et al. (2010) Deubiquitinase USP9X stabilizes MCL1 and promotes tumour cell survival. *Nature* 463(7277):103–107.
34. Song X-T, et al. (2008) A20 is an antigen presentation attenuator, and its inhibition overcomes regulatory T cell-mediated suppression. *Nat Med* 14(3):258–265.
35. Li W, Ye Y (2008) Polyubiquitin chains: Functions, structures, and mechanisms. *Cell Mol Life Sci* 65(15):2397–2406.
36. Xu M, Skaug B, Zeng W, Chen ZJ (2009) A ubiquitin replacement strategy in human cells reveals distinct mechanisms of IKK activation by TNFalpha and IL-1beta. *Mol Cell* 36(2):302–314.
37. Lin JT, et al. (2009) Naive CD4 T cell proliferation is controlled by mammalian target of rapamycin regulation of GRAIL expression. *J Immunol* 182(10):5919–5928.
38. Goncharov T, et al. (2013) OTUB1 modulates c-IAP1 stability to regulate signalling pathways. *EMBO J* 32(8):1103–1114.
39. Myers MD, et al. (2006) Src-like adaptor protein regulates TCR expression on thymocytes by linking the ubiquitin ligase c-Cbl to the TCR complex. *Nat Immunol* 7(1):57–66.
40. Paolino M, Penninger JM (2010) Cbl-b in T-cell activation. *Semin Immunopathol* 32(2): 137–148.
41. Shamim M, et al. (2007) Cbl-b regulates antigen-induced TCR down-regulation and IFN-gamma production by effector CD8 T cells without affecting functional avidity. *J Immunol* 179(11):7233–7243.
42. Zhang J, et al. (2002) Cutting edge: Regulation of T cell activation threshold by CD28 costimulation through targeting Cbl-b for ubiquitination. *J Immunol* 169(5):2236–2240.
43. Claessen JHL, et al. (2013) Catch-and-release probes applied to semi-intact cells reveal ubiquitin-specific protease expression in *Chlamydia trachomatis* infection. *ChemBioChem* 14(3):343–352.
44. Sanyal S, Claessen JHL, Ploegh HL (2012) A viral deubiquitylating enzyme restores dislocation of substrates from the endoplasmic reticulum (ER) in semi-intact cells. *J Biol Chem* 287(28):23594–23603.
45. Sanyal S, et al. (2013) Type I interferon imposes a TSG101/ISG15 checkpoint at the Golgi for glycoprotein trafficking during influenza virus infection. *Cell Host Microbe* 14(5):510–521.
46. Swee LK, et al. (2013) Sortase-mediated modification of αDEC205 affords optimization of antigen presentation and immunization against a set of viral epitopes. *Proc Natl Acad Sci USA* 110(4):1428–1433.
47. Wu J, et al. (2013) Cyclic GMP-AMP is an endogenous second messenger in innate immune signaling by cytosolic DNA. *Science* 339(6121):826–830.
48. Roux KJ, Kim DI, Raida M, Burke B (2012) A promiscuous biotin ligase fusion protein identifies proximal and interacting proteins in mammalian cells. *J Cell Biol* 196(6): 801–810.
49. Roux KJ, Kim DI, Burke B (2001) *BioID: A Screen for Protein–Protein Interactions* (Wiley, Hoboken, NJ).
50. Ernst R, et al. (2011) Enzymatic blockade of the ubiquitin-proteasome pathway. *PLoS Biol* 8(3):e1000605.
51. Balagopalan L, et al. (2011) Enhanced T-cell signaling in cells bearing linker for activation of T-cell (LAT) molecules resistant to ubiquitylation. *Proc Natl Acad Sci USA* 108(7):2885–2890.
52. Mukhopadhyay D, Riezman H (2007) Proteasome-independent functions of ubiquitin in endocytosis and signaling. *Science* 315(5809):201–205.
53. Py BF, Kim M-S, Vakifahmetoglu-Norberg H, Yuan J (2013) Deubiquitination of NLRP3 by BRCC3 critically regulates inflammasome activity. *Mol Cell* 49(2):331–338.
54. van der Veen AG, Ploegh HL (2012) Ubiquitin-like proteins. *Annu Rev Biochem* 81(1): 323–357.
55. Komander D, Clague MJ, Urbé S (2009) Breaking the chains: Structure and function of the deubiquitinases. *Nat Rev Mol Cell Biol* 10(8):550–563.
56. Malissen B, Grégoire C, Malissen M, Roncagalli R (2014) Integrative biology of T cell activation. *Nat Immunol* 15(9):790–797.
57. Poalas K, et al. (2013) Negative regulation of NF-κB signaling in T lymphocytes by the ubiquitin-specific protease USP34. *Cell Commun Signal* 11(1):25.
58. Joo H-Y, et al. (2011) Regulation of histone H2A and H2B deubiquitination and *Xenopus* development by USP12 and USP46. *J Biol Chem* 286(9):7190–7201.
59. Sowa ME, Bennett EJ, Gygi SP, Harper JW (2009) Defining the human deubiquitinating enzyme interaction landscape. *Cell* 138(2):389–403.
60. Kirchgessner H, et al. (2001) The transmembrane adaptor protein TRIM regulates T cell receptor (TCR) expression and TCR-mediated signaling via an association with the TCR zeta chain. *J Exp Med* 193(11):1269–1284.
61. Nurieva RI, et al. (2010) The E3 ubiquitin ligase GRAIL regulates T cell tolerance and regulatory T cell function by mediating T cell receptor-CD3 degradation. *Immunity* 32(5):670–680.
62. Cong L, et al. (2013) Multiplex genome engineering using CRISPR/Cas systems. *Science* 339(6121):819–823.